Hernández-Paniagua, I. Y., Lowry, D., Clemitshaw, K. C., Palmer, P. I., Fisher, R. E., France, J. L., Mendoza, A., O'Doherty, S., Forster, G., Lanoisellé, M., & Nisbet, E. G. (2018). Diurnal, seasonal, and annual trends in tropospheric CO in Southwest London during 2000–2015: Wind sector analysis and comparisons with urban and remote sites. *Atmospheric Environment*, *177*, 262-274. https://doi.org/10.1016/j.atmosenv.2018.01.027

Diurnal, seasonal, and annual trends in tropospheric CO in Southwest London during 2000-2015: Wind sector analysis and comparisons with urban and remote sites

Iván Y. Hernández-Paniagua[1,2,3], David Lowry[1], Kevin C. Clemitshaw[1], Paul I. Palmer[4], Alberto Mendoza[3], Rebecca E. Fisher[1], James L. France[1,5,6], Simon O'Doherty[7], M. Lanoisellé[1] and Euan G. Nisbet[1]*

[1]Department of Earth Sciences, Royal Holloway, University of London, Egham, Surrey, TW20 0EX, United Kingdom.
[2]Centro de Ciencias de la Atmósfera, Universidad Nacional Autónoma de México, México.
[3]Escuela de Ingeniería y Ciencias, Tecnologico de Monterrey, Av. Eugenio Garza Sada 2501, Monterrey, Nuevo León, México, C.P. 64849.
[4]School of GeoSciences, University of Edinburgh, Alexander Crum Brown Road, Edinburgh, EH9 3FF, United Kingdom.
[5]School of Environmental Sciences, University of East Anglia, Norwich NR4 7TJ, United Kingdom.
[6]British Antarctic Survey, High Cross, Cambridge, UK, CB3 0ET.
[7]School of Chemistry, University of Bristol, Cantock's Close, Bristol, BS8 1TS, United Kingdom.

*Corresponding author: e.nisbet@es.rhul.ac.uk.

Highlights

1. CO data recorded at Egham (EGH) in Southwest London during 2000-2015 were analysed.
2. CO varies on time scales ranging from minutes to inter-annual and annual cycles.
3. CO declined more slowly than in Central London.
4. The largest decline rates were observed for the calm and Eastern wind sectors.
5. The assessment of CO/CO_2 residuals confirmed a clear decline in CO during periods of increased vehicle traffic from 2000 to 2015.

Abstract

Ambient CO and meteorological parameters have been measured at the Egham (EGH) semi-rural site in SW London between 2000 and 2015 allowing wind sector analysis of diurnal and seasonal cycles, and interpretation of long-term trends. CO daily amplitudes are used as a proxy for anthropogenic emissions. At EGH, morning and evening peaks in CO arise from the dominant contribution of road transport sources. Smaller amplitudes are observed during mornings and weekends than during evenings and weekdays due to the stability of the night-

time planetary boundary layer. A wavelet transform revealed that the dominant mode of CO variability is the annual cycle, with an apparent winter maxima likely due to increased CO emissions from domestic heating with summer minima ascribed to enhanced dispersion.

Successful CO mitigation measures over the last 25 years have seen a change from the dominance of local diurnal sources to a site measuring close to Atlantic background levels in summer months. The EGH CO record shows the highest levels in the early 2000s, with levels in E and calm winds comparable to those recorded at background stations in Greater London. However, since 2012, levels in S-SW sector have become more comparable with Mace Head background except during rush-hour periods. Marked declines in CO are observed during 2000-2008 for the NE, E, SE (London) and calm wind sectors, with the smallest declines observed for the S, SW and W (background) sectors. For the majority of wind sectors, the decline in CO is less noticeable since 2008, with an apparent stabilisation for NE, E and SE after 2009. The EGH CO data record exhibits a similar but slower exponential decay than do CO data recorded at selected monitoring sites in urban areas in SE England. CO/CO_2 residuals determined using a 1 h window data in the diurnal cycle demonstrate a clear decline in CO from 2000 to 2015 during daily periods of increased vehicle traffic, which is consistent with a sustained reduction in CO emissions from the road transport sector.

Keywords
Combustion emission ratio, exponential decay, road transport, spectral analysis.

1. Introduction

CO is emitted into the troposphere primarily as a product of incomplete combustion processes, including burning of fossil fuels, bio-fuels, and agricultural biomass (Fortems-Cheiney et al., 2011; Worden et al., 2013). In the troposphere, CO is formed by the oxidation of volatile organic compounds (VOCs), and plays a central role in tropospheric chemistry via its reaction with the OH radical to form CO_2 (Waibel et al., 1999; Bergamaschi et al., 2000; Jenkin and Clemitshaw, 2000). Reduction in global CO may indirectly affect the climate by changing the atmospheric life-time of CH_4, which is also oxidised via reaction with OH (IPCC, 2013). The global budget for CO is estimated between 2.2-2.5 PgC yr^{-1}, with around 65% of anthropogenic origin. Annual CO emissions are estimated between 500 and 750 Tg from large-scale biomass burning, between 500 and 650 Tg from fossil and domestic fuel burning, between 700-800 Tg from CH_4 oxidation and around 100 Tg from natural sources (Bergamasschi et al., 2000; Holloway et al., 2000; Duncan et al., 2007; IPCC, 2007; Lin et al., 2008).

CO has an average life-time in the troposphere of around 2 months, although it is seasonally dependent, and may range from 10-30 days in tropical regions during summer, to 90 days and almost 12 months in high northern latitudes (Novelli et al., 1998; Staudt et al., 2001; Zhang et al., 2011). The hemispheric imbalance of higher CO mixing ratios in the Northern Hemisphere (NH) results in spatial and temporal variations, which can be compounded by changes in combustion emissions, long-range transport and natural events such as wildfires. For example, data recorded at background and marine sites at mid-northern latitudes exhibit stronger seasonality (large seasonal amplitude values, AV_s) than at sites in the Southern Hemisphere (SH) (Derwent et al., 1998; Novelli et al., 1998). The highest concentrations of CO are observed typically close to combustion sources (Yurganov et al, 2010), and therefore CO can be used as a proxy for local and regional air pollution, fossil fuel and biomass burning (Edwards et al., 2006).

During the last century, the atmospheric burden of CO varied significantly between decades. For instance, industrialisation in western nations during 1950-1980 resulted in an average global growth rate of around ~1 % CO yr^{-1} (1-2 ppb CO yr^{-1}) due to increased fossil fuel combustion (Zander et al., 1989; Yurganov et al., 1999). Since the 1990s, the introduction of policies to control CO emissions from vehicular sources in Europe and North America have decreased ambient CO by between 10-50 % in urban areas (Kuebler et al., 2001; Bigi and Harrison, 2010; von Schneidemesser et al., 2010), while rural and semi-rural areas experienced reductions of 5-25 % (0.1-10 ppb CO yr^{-1}) (Simmonds et al., 1997; Lin et al., 2008; Worden et al., 2013; Kumar et al., 2013). By contrast, rapid economic development of Asian nations since the 1990s has greatly increased CO emissions, which compensate globally for emissions reduction in Europe and North America (Kumar et al., 2013).

CO emissions in England decreased by around 75 % during 1990-2014, driven mostly by changes in road transport (NAEI, 2016). The major benchmark was the requirement for new petrol cars to be fitted with three-way catalysts since 1989, and the switch in fuel from petrol to diesel. Data recorded within the London Air Quality Network (LAQN) in Greater London show a marked decline in ambient CO, which confirms the inventory trends (LAQN, 2016). For instance, von Schneidemesser et al. (2010) reported a decline in CO at the LAQN Marylebone Road site during 1998-2008 of 12 % yr^{-1}, from 1.6 to 0.53 ppm CO. At the LAQN North Kensington site, Bigi and Harrison (2010) observed a smaller decline of around 3 % yr^{-1} in CO during 1996-2008. More recently, Lowry et al. (2016) reported a marked decline in CO levels during 1997-2014, for air masses arriving at the semi-rural Egham site (EGH) having passed over Greater London, which was ascribed to the adoption of stringent control emissions.

Nevertheless, road transport sources remain a major driver of diurnal variations of CO in the London area (NAEI, 2016). Worldwide, average CO diurnal cycles typically show morning and evening peaks, with a delay of 1-3 h from the rush-period. For instance, within urban and sub-urban areas of Beijing (Xu et al., 2011), Mexico City (Stephens et al., 2008), Seoul (Nguyen et al., 2010) and London (Bigi and Harrison, 2010), the morning peak normally occurs around 08:00-09:00 local time. Ambient CO decreases by mid-day due to reduced emissions and the growth of the planetary boundary layer (PBL) (Shaw et al., 2007). Reduced fossil fuel combustion in the road transport sector during weekends leads to lower levels of CO than during weekdays (Stephens et al., 2008; Grant et al., 2010b). However, diurnal profiles of CO are also affected by seasonal changes of emissions from residential heating and energy-production, variations in the development of the PBL, and changes in wind direction and speed (Helfter et al., 2011; Hernández-Paniagua et al., 2015).

Long-term trends in tropospheric CO have been studied extensively worldwide. However, to date, few studies have addressed diurnal, seasonal and annual variations at a site with contributions from local and regional sources of CO. This study presents 16-years of continuous, high-precision measurements of CO made at the EGH site in SW London. In order to assess local and regional sources, CO levels in air masses that have travelled over Greater London are compared with background levels during westerly Atlantic winds. Daily and seasonal cycles, and long-term annual trends in CO at EGH are compared with those observed at selected sites within the UK Automatic Urban and Rural Network (AURN) and LAQN. Furthermore, CO data recorded during westerly winds are contrasted with those recorded at the Mace Head (MHD) observatory on the west coast of Ireland to estimate local rates of change as result of air quality control policies.

2. Experimental

2.1. Sampling location

High-precision and high-frequency in-situ measurements of tropospheric CO were made during 2000-2015 at the Greenhouse Gas Laboratory of the Department of Earth Sciences (ES) at the EGH campus of Royal Holloway University of London. The EGH site is situated in Surrey, UK (51° 25’ 36” N, 0° 33’ 40” W), some 32 km WSW of Central London (Fig. 1a), and approximately 8 km SW of London Heathrow Airport, 1.8 km W of the M25 motorway, and 1 km SW of the town of Egham (Fig. 1b). Around 2 km W of EGH lies Windsor Great Park, which is a mix of forested and agricultural land, and covers an area of some 30 km^2. The SW sector is mostly sub-urban, with houses scattered between predominant woodland, while the E sector is dominated by Greater London. Further details of the EGH site have been provided recently (Hernández-Paniagua et al., 2015; Lowry et al., 2016).

2.2. CO measurement methodology, instrumentation and calibration

CO was measured in air sampled approximately 15 m above ground level via an air inlet manifold 3 m above the roof of the ES building. This single length of ½-inch OD Synflex tubing enters the laboratory and is connected to a KNF-Neuberger pump which draws in air at a flow rate of 20 L min^{-1}. After the pump, the air inlet splits to feed a suite of measurement instruments. Until the end of 2008, CO measurements were made every 30-mins with a Trace Analytical Reduction Gas Detector (RGD-2) instrument, precise to ±2 ppb CO, using two 1/8" packed columns in series: a Unibeads 1S and a Molecular Sieve 5A, with zero air as the carrier gas. Working standards were calibrated twice per month using NOAA CMDL-filled and analysed cylinders of ambient air within the range 168-304 ppb CO (Lowry et al., 2016).

Since January 2008, the monitoring of CO was improved with the installation of a Peak Performer Analyser 1 (PP1) reduced compound photometer, with columns and carrier gas as for the RGD-2. Measurements were made every 5-mins with a stated precision better than ±1 ppb CO. A working standard was measured twice daily with twice monthly calibration checks using a suite of NOAA CMDL-filled and analysed cylinders of ambient air containing 186-300 ppb CO. The RGD-2 and PP1 instruments were run simultaneously during 2008 to inter-compare measurements, with data in very good agreement in the range 80-600 ppb CO, and a post-calibration offset of 0±5 ppb CO, a correlation gradient of 0.92, an intercept of 14.45 ppb CO, an r value of 0.98 and $p<0.001$. Since 2008, the PP1 has been the primary source of CO data. Further details can be found elsewhere (Lowry et al., 2016).

CO data capture varied between 78-99% of the annual maximum despite occasional instrument downtime. Figure 2 shows data capture for 30-min CO averages recorded during 2000-2015. CO daily averages were calculated from 30-min data; monthly averages from CO daily averages, with annual averages derived from CO monthly averages. Data capture for wind speed ranged from 67-99%, for wind direction 76-99% and for air temperature, 88-99% (Fig. 2).

2.3. AURN, LAQN and Mace Head (MHD) CO data sets

The AURN is the UK's largest automatic monitoring network with data used to assess compliance against Objectives of the UK and EU Ambient Air Quality Directives (Defra, 2017). Currently, 136 monitoring sites are operative and perform measurements of ambient NO and NO_2 (collectively NO_x), sulphur dioxide (SO_2), ozone (O_3), CO and particulate matter (PM_{10} and $PM_{2.5}$) across the UK (Defra, 2017). Quality assurance and quality control (QA/QC) processes for the AURN data are carried out independently by Ricardo Energy & Environment.

Hourly AURN CO data, valid with a minimum data capture of 90%, were obtained from the AURN web site (Table 1) (http://uk-air.defra.gov.uk/data). Hourly LAQN CO data, valid with a minimum data capture of 75%, were downloaded from the LAQN web site (Table 1) (http://www.londonair.org.uk/london/asp/datadownload.asp) (LAQN, 2016).

The MHD research station is located on the west coast of Ireland (53°20' N, 9°54' W), which is ideal to monitor Atlantic background air masses. Further details of the MHD site are provided in Derwent et al. (2002) and Messager et al. (2008). The MHD CO dataset is maintained by the University of Bristol as part of the UK DECC Network and Advanced Global Atmospheric Gases Experiment (AGAGE), and was obtained from the web site of the World Data Centre for Greenhouse Gases (WDCGG) of the World Meteorological Organisation (WMO) (http://ds.data.jma.go.jp/gmd/wdcgg). It currently spans continuous measurements of CO made from March 1994 to September 2013.

2.4. Meteorology at EGH and wind sector and seasonal analyses

The climate at EGH is maritime and mild, with significant month-to-month variations in wind direction and speed during the year (Figure 3) (Hernández-Paniagua et al., 2015; Lowry et al., 2016). SW winds are most common as depressions track across the UK, whereas E winds are frequent during anti-cyclonic conditions. Relatively clean air arrives at EGH from the SW and SSW. By contrast, E air masses trajectories pass over Greater London (8.17 million people; ONS, 2011) before arrival at EGH. During slow-moving anti-cyclonic air conditions in winter and early spring, the initial relatively clean air is augmented by combustion emissions from the London basin. Figure 3 shows that overall during 2000-2015, the predominant wind direction at EGH was SW, occurring between 17.9 and 24.7 % of the time in spring and winter, respectively. The largest frequency of high wind speeds is observed for winter and contrasts with the lowest frequency of calm events observed 11.5 % of the total time.

To perform wind-sector analyses, the EGH dataset was divided into 8 wind sectors of 45° starting from 0° ± 22.5° and an additional calm category (<0.1 m s^{-1}). The lower bound of each sector was established by adding 0.5° to avoid data duplicity. Seasons were defined according to temperature records in the NH: winter (December to February), spring (March to May), summer (June to August) and autumn (September to November).

2.6. Mathematical analyses

The CO data sets were analysed extensively with the *openair* package (Carslaw and Ropkins, 2012; Carslaw and Beevers, 2013) for R software (R Core Team, 2013). Long-term trends were computed as described previously (Hernández-Paniagua et al., 2015), with the

MAKESENS 1.0 macro (Salmi et al., 2002) used to test the presence of a statistically significant monotonic linear trend. MAKESENS relies on the non-parametric Mann-Kendall test to estimate the slope and intercept of a linear trend, which is quantified with the non-parametric Sen's method. Long-term trends from the MAKESENS macro were compared with those obtained with the Theil-Sen tool included in the *openair* package. All results presented here did not show statistical differences (p>0.05) between both tests.

Seasonal cycles, secular trends and residual components were computed using the seasonal-trend decomposition technique (STL) developed by Cleveland et al. (1990) as described previously (Hernandez-Paniagua et al., 2015). Statistical analyses were performed with the computational software SPSS 19.0 for Microsoft Windows.

3. Results and discussion

3.1 Time-series in CO recorded at EGH during 2000-2015

The EGH CO dataset exhibits recurrent seasonal cycles and pollution episodes, and a clear sustained decline in the maximum observed values from 2000 to 2008 (Fig. 4). High CO mixing ratios, >1000 ppb, were frequently recorded before 2008, mostly during winter, with lowest values recorded during summer. Table 2 provides annual descriptive statistics for the entire dataset. By the early 2000s, the CO levels (> 400 ppb) recorded in E and calm winds arriving at EGH are similar to those recorded at North Kensington and Marylebone Rd in Central London (Bigi and Harrison, 2010; von Schneidemesser et al., 2010). By contrast, the annual average CO levels observed for the S-SW sectors at EGH since 2012 are not far above the overall averages measured at MHD (Lowry et al., 2016). In addition to this pronounced decline, winter-time pollution episodes have also decreased in severity. Satellite measurements of decreasing tropospheric CO over Europe agree with the apparent decline of CO observed in EGH, which is also observed above North America (Yurganov et al., 2010; Fortems-Cheiney et al., 2011; Pommier et al., 201; 3Worden et al., 2013; Lowry et al., 2016).

3.2 Daily and weekly cycles of CO at EGH

Diurnal variations in CO arise from changes in emissions from combustion sources and changes in meteorology, mostly in the PBL height (Grant et al., 2010b; Hossain et al., 2012; Defra, 2017). Figure 5 shows normalised daily cycles for CO at EGH, derived from hourly averages, by season and day of the week during 2000-2015. Peak-to-trough amplitude values of the CO diurnal cycles (AV_d) were calculated for morning and evening peaks for weekends and weekdays to assess diurnal variations in CO emissions. The morning and evening peaks in CO observed at EGH arise from the dominant contribution of road transport sources to the daily cycle as discussed by Bigi and Harrison (2010). By contrast, monitoring sites that

experience air masses with relatively minor combustion sources of CO typically exhibit a single PBL-related CO peak in the daily cycle (An et al., 2013).

Overall, at EGH, morning AV_d values are lower than evening values for all seasons, with Sunday values the lowest of the week. This is in good agreement with traffic data for Greater London that shows the greatest traffic volume typically occurring during weekdays between 16:00-18:00 GMT (DfT, 2016). Differences of around 1 to 3 h between the maximum traffic volume and the peak occurrence in CO can be ascribed to the time required for emissions to mix, dilute and disperse from sources closer to London. Grant et al. (2010b) reported from semi-continuous measurements of CO and H_2 made at the city centre of Bristol UK, that the stability of the PBL height overnight affects the dispersion of evening CO emissions, and thus explains their persistence.

3.3 CO annual cycles at EGH

To identify and isolate seasonal features, a wavelet transform was used to spectrally decompose the EGH CO dataset (Torrence and Compo, 1998). As described previously (Barlow et al., 2015), this method preserves frequency variations as a function of time, and allows for the time evolution of signals. It has been applied to Arctic CO_2 (Barlow et al., 2015), CO (Mackie et al., 2016), and CH_4 (Barlow et al., 2016). Figure 6 shows the power spectrum of the CO data which were normalised to reduce the magnitude of their values and thereby permit data to be decomposed and reconstructed to within less than 1% of the original.

The dominant mode of CO variability is the annual cycle, as anticipated from inspection of the raw data. While the global power spectrum is strongly peaked at one year, the power is spread across neighbouring periods, reflecting the high resolution of the data. Consequently, periods of 10 to 15 months are conservatively added to the annual cycle; previous analysis of CO mixing ratios (Mackie et al., 2016) used 6-18 months to represent the annual cycle of lower resolution weekly data. Using the wavelet transform as a band-pass filter isolates a subset of periods, e.g., to de-seasonalise the data by retaining periods >15 months. Overall, Fig. 6 shows that the amplitude of the CO seasonal cycle, and the low- and high-frequency variations, all diminish with time from 2000.

The annual cycle of CO arises from seasonal changes in OH concentration, anthropogenic emissions and meteorological conditions (Novelli et al., 1998; Kim et al., 2011). To determine typical maxima and minima occurrence in CO at EGH, de-trended average annual CO cycles by wind sector were obtained by subtracting annual averages from each monthly average,

which removes the impact of long-term trends (Fig. 7). The average annual CO cycles at EGH exhibit an apparent winter maxima and summer minima, in agreement with other studies in the NH (Simmonds et al., 1997; Derwent et al., 1998; Novelli et al., 1998; Bigi and Harrison, 2010; Makarova et al., 2011; Kim et al., 2011). Since vehicular emissions of CO remain fairly constant throughout the year, increased CO emissions from domestic heating together with a decrease in the PBL height may contribute to the elevated mixing ratios observed during winter for all wind sectors (NAEI, 2016).

The occurrence of frequent E and NE air masses at EGH that potentially transport CO emitted from Greater London are likely to cause the largest peaks observed during winter for those wind sectors. Calm periods give the highest mixing ratios between January-March, which may arise from stable atmospheric conditions and frequent inversions that prevent local CO emissions from dispersing. This can be confirmed by the lowest CO mixing ratios observed for the background S and SW sectors, which suggests a low contribution from other CO sources during winter. By contrast, the lowest CO mixing ratios are observed during summer for all wind sectors, with the largest amplitude detected for calm and the lowest for the background sector. This can be ascribed to enhanced convective conditions in summer, which promote dispersion of CO emissions, in combination with dilution by mixing with clean S and SW air masses (Grant et al., 2010b).

3.4 Wind sector analysis of long-term trends in CO at EGH

The secular trends of CO at EGH by wind sector during 2000-2015 were calculated from annual averages, derived from monthly averages filtered with the STL technique (Cleveland et al., 1990). The best fitting for the whole EGH CO data record is given by an offset exponential function as reported by Lowry et al. (2016). Figure 8 shows exponential fittings for all wind sectors at EGH and the parameterisation of the trends. Overall, marked declines in CO are observed during 2000-2008 for the NE, E, SE and calm, with the lowest declines observed for the S, SW and W wind sectors. For the majority of wind sectors, the decline in CO is less noticeable since 2008, with an apparent stabilisation for NE, E and SE after 2009. When the trends in CO are linearised with the Mann-Kendall approach, the declines for all wind sectors are significant at $p<0.001$ as listed in Table 3. The linear declines range from 4.7 ppb CO yr^{-1} (2.4 % yr^{-1}) to 18.7 ppb CO yr^{-1} (4.8 % yr^{-1}) for S and E wind sectors, respectively. As in the exponential fitting, the largest declines correspond to the NE, E, SE and calm winds sectors, with decreases in CO of 60.8-76.8 % during 2000-2015.

The decline rates in CO of 4.7 and 5.9 ppb CO yr^{-1} observed for the S and SW wind sectors at EGH (Table 3) are consistent with the 2.65 ± 0.04 ppb CO yr^{-1} recorded during 1991-2004

at Jungfraujoch, Switzerland (Zellweger et al., 2009), but considerably greater than the 0.84 ± 0.95 ppb CO yr^{-1} recorded at Zugspitz, Germany during 1991-2004 (Chevalier et al., 2008). At EGH, CO levels in SW and S air masses are close to Atlantic CO values because of relatively few significant CO emissions sources over SW England. This explains the lowest decline rates in CO observed for such wind sectors, and is ascribed to the abatement of more minor CO emission sources than those observed for the urban sectors. By contrast, the large declines in CO for the NE, E and calm wind sectors (the London sectors) are significantly lower than that at North Kensington of ca. 50 ppb CO yr^{-1} during 1996-2008 (Bigi and Harrison, 2010), and represent around 15 to 20 % of that of ca. 98 ppb yr^{-1} at Marylebone Rd during 1998-2008 (von Schneidemesser et al., 2010). Kuebler et al. (2001) reported larger CO decline rates for urban sites than for rural sites over Switzerland, which is in agreement with the decline rates observed for the different wind sectors at EGH. This is consistent with the rapid abatement of large CO sources such as road transport, followed by a slower reduction in the remaining sources (Lowry et al., 2016; NAEI, 2016).

3.5 Decline of CO in the London area and comparison with the UK NAEI

EGH trends are compared with those estimated for representative long-term sites within Greater London to put the decline in CO estimated at EGH in the context of SE England. Figure 9 shows the comparison of trends in CO for LAQN sites over Greater London and the urban centre Reading (REA) (around 30 km NW of EGH), with representative EGH wind sectors during 2000-2015. Note the difference in scale for MY1. The LAQN/AURN CO trends follow an exponential decay and can be represented by the exponential function proposed for EGH by Lowry et al. (2016) with fittings ranging from R^2 = 0.74 for KC1 to R^2 = 0.96 for REA (Supplementary Information, Table S1). Parameterisation of the trends from 2000 to 2015 indicates the largest decline occurred at MY1 (78 %, i.e. 4.9 % yr^{-1}) with the smallest decline at LH2 (16 %, i.e. 1.0 % yr^{-1}). Annual declines in CO at MY1 and KC1 of ca. 12 % yr^{-1} and 3 % yr^{-1} during 1998-2008 and 1996-2008, respectively (von Schneidemesser et al. (2010); Bigi and Harrison, 2010), are around 2.5-3 times greater than those determined here for such sites from 2000 to 2015. The differences in CO declines arise from assessment of different time periods, and are consistent with effective abatement of large CO sources during the late 1990s and early 2000s, as evidenced by the large declines observed for LH2 and REA during 2000-2007.

The CO declines for the LAQN/AURN sites assessed during 2000-2015 agree with those observed for the EGH NE, E and calm wind sectors but differ significantly from the EGH S and SW wind sectors. The UK NAEI reports an overall decline in CO emissions of 59 % from 2000 to 2014. This decline followed two major changes in the vehicle fleet. The first was legislation

in the 1990s for more rigorous control on exhaust emissions from petrol-fuelled vehicles, coupled with tax switches to make leaded petrol more expensive than unleaded (hence reducing poisoning of exhaust catalysts by leaded fuel). Secondly, there has been a sharp increase in diesel vehicles, which emit much less CO, that previously were a small proportion but now comprise half of new cars sold. While this has caused very damaging pollution from NO_x emissions, it has reduced CO emission.

Figure 10a shows that the largest reduction in CO emissions is for road transport, which is estimated at around 84 % (5.6 % yr^{-1}) during 2000-2014 (NAEI, 2016), and is similar to that reported here for MY1 kerbside site during 2000-2015. Although, CO emissions from the road transport sector still remain significant, currently, the largest reported source is stationary combustion. Figure 10b shows that CO recorded at EGH for E and calm wind sectors decrease in a similar way as NAEI CO emissions estimates. The increase in CO observed in 2010 is likely due to cold weather experienced during winter as reported by the UK NAEI (2016), which triggered CO stationary combustion emissions from the residential sector. It is also possible that a 4-fold increase in the use of biomass for industrial combustion since 2008 may have offset reductions in emissions from other sources (NAEI, 2016).

3.6 Mace Head comparison

Figure 11 compares normalised CO daily cycles at EGH and MHD during 2000-2013, calculated from hourly averages relative to the daily average. Larger peak-to-trough amplitudes are evident at EGH than at MHD, especially during 2000-2008. The largest apparent decline in CO amplitudes at EGH is observed for the morning peak and E wind sector. By 2013, the daily cycles for SW EGH wind sector are close to those observed at MHD, although a morning peak at EGH is still apparent. The larger amplitudes in CO at EGH arise from emission of significant CO sources in SE England, which are absent at MHD. Both, the morning and evening CO peaks coincide with the traffic rush hours, which suggests a large contribution of road transport sources not detected at MHD (An et al., 2013).

The long-term trend in CO at MHD during 2000-2013 calculated from de-seasonalised annual averages determined from the whole data set is compared with those estimated at EGH for E, SW, calm and all wind sectors from 2000 to 2015, and are shown in Fig. 12. CO at MHD shows a significant (p<0.05) increasing linear trend of 0.84 ppb CO yr^{-1} in marked contrast with the exponential declines for CO recorded at EGH. The increasing trend at MHD is opposite to that observed at the Pico Mountain Observatory (PMO) in the Azores of -0.31 ppb yr^{-1} during 2001-2011 (Kumar et al., 2013), which was ascribed to decrease in CO anthropogenic emissions from North America. Grant et al. (2010a) reported that in European polluted air masses at

MHD, background levels of hydrogen increase on average 5.3 ppb, likely due to the transport of primary emissions from fossil fuel combustion. Such continental transport could explain the increasing trend in CO at MHD, which is not observed at the PMO because of the small influence from European air masses. Although by 2013, CO at EGH and MHD are comparable during SW air masses, CO levels at EGH for E and calm wind sectors exceed MHD values by 84 and 76 ppb, respectively, despite significantly reduced CO emissions in SE England since 2000 (NAEI, 2016).

3.7 CO/CO_2 ratio

The ratio of CO/CO_2 provides further insight into changes in combustion emissions of CO as it is not affected by dilution processes due to boundary layer dynamics (Chandra et al., 2016). To assess the decrease in road transport emissions of CO, the CO/CO_2 residual was defined as the excess CO/CO_2 in air from NE-E wind sectors compared with the S wind sector. Further details of the EGH CO_2 record can be found elsewhere (Hernández-Paniagua et al., 2015). Figure 13 shows diurnal variations of CO/CO_2 residuals during 2000-2015 using a 1 h window data in the diurnal cycle for 4 periods of 3-yr, and for 2012-2015. The CO/CO_2 residuals demonstrate a clear decline in CO from 2000 to 2015 during periods of increased vehicle traffic, with the largest declines during 2000-2008. Table S2 lists cumulative declines in CO/CO_2 daily residuals. Overall, during the whole period, declines of 72 and 75 % are observed for the maxima and average CO/CO_2 daily residuals, respectively, although a decline of 91 % is observed for the minima CO/CO_2 daily residuals. These declines are consistent with the sustained reduction in CO emissions from the road transport sector, and with the early abatement of larger CO sources followed by a more difficult reduction in remaining sources (NAEI, 2016).

4. Conclusions

Long-term trends for CO data recorded at EGH from 2000 to 2015 are addressed using a wind sector analysis, traffic and emissions data, as well as comparison with urban and remote monitoring sites. CO varies on time scales ranging from hourly to daily at EGH, with seasonal and inter-annual cycles. CO 1-h mixing ratios recorded during 2000-2008 have declined clearly in magnitude, simultaneously with the occurrence of severe episodes. Since 2010, the largest 1-h CO mixing ratios measured are similar to the lowest ones observed in the early 2000s. Diurnal cycles in CO are driven by the PBL height and changes in road transport emissions. CO seasonal cycles arise from changes in meteorological conditions and emissions, with winter maxima coincident with the greatest emissions from stationary combustion and minima occurring under conditions of enhanced convection.

The wind sector analysis carried out revealed that the largest CO mixing ratios are measured in air masses from the E and NE, which arrive at EGH after passing over Greater London and Heathrow airport. By contrast, the lowest CO mixing ratios are recorded for air masses from the S and SW wind sectors. The long-term trend in CO at EGH follows an exponential decay, with the largest rate of change observed during 2001-2008, and for the NE, E and calm wind sectors. Linearised trends in CO from 2000 to 2015 suggest declines of 4.7 and 18.7 ppb yr^{-1} for S and E wind sectors, respectively. The declines in CO for the urban wind sectors follow the exponential decrease observed for monitoring sites in Greater London, although the latter declines more rapidly.

When compared with CO recorded at MHD, the EGH CO mixing ratios are significantly higher with larger daily amplitudes in response to road transport emissions. From 2000 to 2013, MHD exhibits an increasing long-term trend, which contrasts with the exponential decline in CO at EGH. The decline in CO recorded at EGH during 2000-2015 comes from the significant decrease in CO emissions, and is consistent with the reduction in emissions from the road transport sector following introduction in the late 1990s of stricter controls by UK and EU legislation to improve air quality, and also, paradoxically, the dieselisation of the car fleet, that otherwise greatly increased pollution. The S-SW sector is now comparable with MHD background except during rush-hour periods. London has a long record of CO pollution (Evelyn, 1772): the progress made with CO in the past two decades demonstrates the feasibility of bringing all pollutants down to near-background levels.

5. Acknowledgements

Grant-aided support to I.Y. Hernández-Paniagua from the Mexican National Council of Science and Technology (CONACYT, scholarship number 215094) and Public Education Ministry (SEP) is gratefully acknowledged. The RHUL Greenhouse Gas Laboratory has been supported by NERC, HEFCE, the EU and RHUL since 1994. P.I.P. gratefully acknowledges support from his Royal Society Wolfson Research Merit Award. The operation of the Mace Head atmospheric station was supported the Department of Business Energy and Industrial Strategy (BEIS, UK) (contract GA0201 to the University of Bristol).

6. References

An, X., Sun, Z., Lin, W., Jin, M., Li, N. (2013). Emission inventory evaluation using observations of regional atmospheric background stations of China. J. Environ. Sci-China, 25(3), 537-546.

Barlow, J.M., Palmer, P.I., Bruhwiler, L.M., Tans, P. (2015). Analysis of CO_2 mole fraction data: first evidence of large-scale changes in CO_2 uptake at high northern latitudes, Atmos. Chem. Phys., 15, 13,739-13,758.

Barlow, J.M., Palmer, P.I., Bruhwiler, L.M. (2016). Increasing boreal wetland emissions inferred from reductions in atmospheric CH_4 seasonal cycle, Atmos. Chem. Phys. Discuss., https://doi.org/10.5194/acp-2016-752, 2016.

Bergamaschi, P., Hein, R., Heimann, M., Crutzen, P.J. (2000). Inverse modeling of the global CO cycle 1. Inversion of CO mixing ratios. J. Geophys. Res., 105(D2), 1909-1927.

Bigi, A., Harrison, R.M. (2010). Analysis of the air pollution climate at a central urban background site. Atmos. Env., 44(16), 2004-2012.

Carslaw, D.C., Ropkins, K. (2012). openair - An R package for air quality data analysis. Environ. Modell. Soft., 27-28, 52-61.

Carslaw, D.C., Beevers, S.D. (2013). Characterising and understanding emission sources using bivariate polar plots and k-means clustering. Environ. Modell. Soft., 40, 325-329.

Carslaw, D.C. (2015). The openair manual - open-source tools for analysing air pollution data. Manual for version 1.0, King's College London.

Chandra, N., Lal, S., Venkataramani, S., Patra, P. K., Sheel, V. (2016). Temporal variations of atmospheric CO_2 and CO at Ahmedabad in western India. Atmos. Chem. Phys., 16(10), 6153-6173.

Chevalier, A., Gheusi, F., Attié, J.L., Delmas, R., Zbinden, R., Athier, G., Counsin, J.M. (2008). Carbon monoxide observations from ground stations in France and Europe and long-term trends in the free troposphere. Atmos. Chem. Phys. Discuss., 8, 3313-3356.

Cleveland, R.B., Cleveland, W.S., McRae, J., Terpenning, I. (1990). STL: a seasonal-trend decomposition procedure based on loess. J. Off. Stats., 6(1), 3-33.

Defra, 2017. Pollutant Information: Carbon Monoxide**.** National Atmospheric Emissions Inventory. Available at: http://naei.defra.gov.uk/overview/pollutants?pollutant_id=4. Last access: 21 Jun 2017.

Department for Transport (DfT). (2016). Road Traffic Statistics. Annual Road Traffic Estimates: Great Britain 2015. Available at: https://www.gov.uk/government/collections/. Last access: 20 Jun 2017.

Derwent, R.G., Simmonds, P.G., Seuring, S., Dimmer, C. (1998). Observation and interpretation of the seasonal cycles in the surface concentrations of ozone and carbon monoxide at Mace Head, Ireland from 1990 to 1994. Atmos. Environ., 32(2), 145-157.

Derwent, R.G., Ryall, D.B., Manning, A., Simmonds, P.G., O'Doherty, S., Biraud, S. (2002). Continuous observations of carbon dioxide at Mace Head, Ireland from 1995 to 1999 and its net European ecosystem exchange. Atmos. Environ., 36(17), 2799-2807.

Duncan, B.N., Logan, J.A., Bey, I., Megretskaia, I.A., Yantosca, R.M., Novelli, P.C., Jones, N. B., Rinsland, C.P. (2007). Global budget of CO, 1988-1997: Source estimates and validation with a global model. J. Geophys. Res., 112(D22301).

Edwards, D.P., Emmons, L.K., Gille, J.C., Chu, A., Attié, J.L., Giglio, L., Wood, S.W., Haywood, J., Deeter, M.N., Massie, S.T., Ziskin, D.C., Drummond, J.R. (2006). Satellite-observed pollution from Southern Hemisphere biomass burning. J. Geophys. Res., 111(D14312).

Evelyn, J. (1772). Fumifugium or, the inconvenience of the aer, and smoake of London dissipated. Together with some remedies humbly proposed by JE Esq; to his sacred Majestie, and To the Parliament now Assembled. Published by His Majesties Command. W. Godbid for G. Bedel and T. Collins. 26pp. Available at: https://quod.lib.umich.edu/e/eebo/A38788.0001.001?c=eebo;c=eebo2;g=eebogroup;rgn=works;view=toc;xc=1;rgn1=author;q1=evelyn. Last access: 1 Aug 2017.

Fortems-Cheiney, A., Chevallier F., Pison I., Bousquet P., Szopa S., Deeter M. N., and Clerbaux C. (2011). Ten years of CO emissions as seen from Measurements of Pollution in the Troposphere (MOPITT). J. Geophys. Res. 116(D05304).

Grant, A., Witham, C. S., Simmonds, P. G., Manning, A. J., O'Doherty, S. (2010a). A 15 year record of high-frequency, in situ measurements of hydrogen at Mace Head, Ireland. Atmos. Chem. Phys., 10(3), 1203-1214.

Grant, A., Stanley, K.F., Henshaw, S.J., Shallcross, D.E., O'Doherty, S. (2010b). High-frequency urban measurements of molecular hydrogen and carbon monoxide in the United Kingdom. Atmos. Chem. Phys., 10(10), 4715-4724.

Helfter, C., Famulari, D., Phillips, G.J., Barlow, J.F., Wood, C.R., Grimmond, C.S.B., Nemitz, E. (2011). Controls of carbon dioxide concentrations and fluxes above central London. Atmos. Chem. Phys., 11(5), 1913-1928.

Hernández-Paniagua, I.Y., Lowry, D., Clemitshaw, K.C., Fisher, R.E., France, J.L., Lanoisellé, M., Ramonet, M., Nisbet, E.G. (2015). Diurnal, seasonal, and annual trends in atmospheric CO_2 in Southwest London during 2000-2012: Wind sector analysis and comparison with Mace Head, Ireland. Atmos. Environ., 105, 138-147.

Holloway, T., H. Levy II, Kasibhatla, P. (2000). Global distribution of carbon monoxide. J. Geophys. Res., 105(D10), 12,123-12,147.

Hossain, K.M.A., Easa, S.M. (2012). Pollutant dispersion characteristics in Dhaka City, Bangladesh. Asia-Pac. J. Atmos. Sci. 48(1), 35-41.

IPCC, 2007: Climate Change 2007: The Physical Science Basis. Contribution of Working Group I to the Fourth Assessment Report of the Intergovernmental Panel on Climate Change [Solomon, S., D. Qin, M. Manning, Z. Chen, M. Marquis, K.B. Averyt, M.Tignor and

H.L. Miller (eds.)]. Cambridge University Press, Cambridge, United Kingdom and New York, NY, USA.

IPCC, 2013: Climate Change 2013: The Physical Science Basis. Contribution of Working Group I to the Fifth Assessment Report of the Intergovernmental Panel on Climate Change [Stocker, T.F., D. Qin, G.-K. Plattner, M. Tignor, S.K. Allen, J. Boschung, A. Nauels, Y. Xia, V. Bex and P.M. Midgley (eds.)]. Cambridge University Press, Cambridge, United Kingdom and New York, NY, USA, 1535 pp.

Jenkin, M.E., Clemitshaw, K.C. (2000). Ozone and secondary photochemical pollutants: Chemical processes governing their formation in the planetary boundary layer. Atmos. Environ., 34(16), 2499-2527.

Kuebler, J., Van Den Bergh, H., Russell, A.G. (2001). Long-term trends of primary and secondary pollutant concentrations in Switzerland and their response to emission controls and economic changes. Atmos. Environ., 35(8), 1351-1363.

Kumar, A., Wu, S., Weise, M.F., Honrath, R., Owen, R.C., Helmig, D., Kramer, L., Val Martin, M., Li, Q. (2013). Free-troposphere ozone and carbon monoxide over the North Atlantic for 2001-2011. Atmos. Chem. Phys., 13(24), 12,537-12,547.

London Air Quality Network (LAQN). (2017). Environmental Research Group, King's College London. Web site: http://www.londonair.org.uk/LondonAir/Default.aspx. Last access: 21 Jun 2017.

Lowry, D., Lanoiselle, M., Fisher, R.E., Martin, M., Fowler, C.M.R., France, J.L., Hernandez-Paniagua, I.Y., Novelli, P.C., Sriskantharajah, S., O'Brien, P., Rata, N.D., Holmes, C.W., Fleming, Z.L., Clemitshaw, K.C., Zazzeri, G., Pommier, M., McLinden, C.A., Nisbet, E.G.. (2016). Marked long-term decline in ambient CO mixing ratio in SE England, 1997-2014: Evidence of policy success in improving air quality. Sci. Rep. 6, 25661.

Lin, Y.C., Lan, Y.Y., Tsuang, B.-J., Engling, G. (2008). Long-term spatial distributions and trends of ambient CO concentrations in the central Taiwan basin. Atmos. Environ., 42(18), 4320-4331.

Mackie, A. R., P. I. Palmer, J. M. Barlow, D. P. Finch, P. Novelli, L. Jaeglé. (2016), Reduced Arctic air pollution due to decreasing European and North American emissions. J. Geophys. Res. Atmos., 121(14), 8692-8700.

Messager, C., Schmidt, M., Ramonet, M., Bousquet, P., Simmonds, P., Manning, A. Ciais, P. (2008). Ten years of CO_2, CH_4, CO and N_2O fluxes over Western Europe inferred from atmospheric measurements at Mace Head, Ireland. Atmos. Chem. Phys. Discuss., 8(1), 1191-1237.

Nguyen, H., Kim, K., Ma, C., Cho, S., Sohn, J. (2010). A dramatic shift in CO and CH_4 levels at urban locations in Korea after the implementation of the natural gas vehicle supply (NGVS) program. Environ. Res., 110(4), 396-409.

Novelli, P.C., Masarie, K.A., Lang, P.M. (1998). Distributions and recent changes of carbon monoxide in the lower troposphere. J. Geophys. Res. D103(15), 19015-19033.

Office for National Statistics (ONS) – 2011 Census: Key Statistics and Quick Statistics for Local Authorities in the United Kingdom. (2013). Available at: https://www.ons.gov.uk/employmentandlabourmarket/peopleinwork/employmentandemployeetypes/bulletins/keystatisticsandquickstatisticsforlocalauthoritiesintheunitedkingdom/2013-12-04. Last access: 21 Jun 2017.

Pommier, M., Mclinden, C. A., Deeter, M. (2013). Relative changes in CO emissions over megacities based on observations from space. Geophys. Res. Lett., 40(14), 3766-3771.

R Core Team. (2013). R: a Language and Environment for Statistical Computing. R Foundation for Statistical Computing, Vienna, Austria, ISBN 3-900051-07-0.

Torrence, C. and Compo, G. P. (1998). A practical guide to wavelet analysis, B. Am. Meteorol. Soc., 79, 61-78.

von Schneidemesser, E., Monks, P.S., Plass-Duelmer, C. (2010). Global comparison of VOC and CO observations in urban areas. Atmos. Environ., 44(39), 5053-5064.

Salmi, T., Määttä, A., Anttila, P., Ruoho-Airola, T., Amnell, T. (2002). Detecting trends of annual values of atmospheric pollutants by the Mann-Kendall test and Sen's slope estimates – the Excel template application MAKESENS. Publications on Air Quality Report code FMI-AQ-31, (31)1-35. Helsinki, Finland.

Shaw, W.J., Pekour, M.S., Coulter, R.L., Martin, T.J., Walters, J.T. (2007). The daytime mixing layer observed by radiosonde, profiler, and lidar during MILAGRO. Atmos. Chem. Phys. Discuss., 7, 15025-15065.

Simmonds, P.G., Seuring, S., Nickless, G., Derwent, R.G. (1997). Segregation and interpretation of ozone and carbon monoxide measurements by air mass origin at the TOR Station Mace Head, Ireland from 1987 - 1995. J. Atmos. Chem., 28(1-3), 45-59.

Staudt, A. C., Jacob, D. J., Logan, J. A., Bachiochi, D., Krishnamurti, T. N., Sachse, G. W. (2001). Continental sources, transoceanic transport, and interhemispheric exchange of carbon monoxide over the Pacific. J. Geophys. Res. 106(D23), 32571-32589.

Stephens, S., Madronich, S., Wu, F., Olson, J. B., Ramos, R., Retama, A., Muñoz, R. (2008). Weekly patterns of México City's surface concentrations of CO, NO_x, PM_{10} and O_3 during 1986-2007. Atmos. Chem. Phys., 8(17), 5313-5325.

UK National Atmospheric Emissions Inventory, NAEI (2016). Air quality pollutant inventories for England, Scotland, Wales and Northern Ireland: 1990 - 2014. A report of the National

Atmospheric Emissions Inventory. Available at: http://naei.defra.gov.uk/. Last access: 21 Jun 2017.

Waibel, A.E., Fischer, H., Wienhold, F.G., Siegmund, P.C., Lee, B., Ström, J., Lelieveld, J., Crutzen, P.J. (1999). Highly elevated carbon monoxide concentrations in the upper troposphere and lowermost stratosphere at northern midlatitudes during the STREAM II summer campaign in 1994. Chemosphere Global Change Sci., 1(1-3), 233-248.

Worden, H.M., Deeter, M.N., Frankenberg, C., George, M., Nichitiu, F., Worden, J., Aben, I., Bowman, K.W., Clerbaux, C., Coheur, P.F., De Laat, A.T.J., Detweiler, R., Drummond, J.R., Edwards, D.P., Gille, J.C., Hurtmans, D., Luo, M., Martínez-Alonso, S., Massie, S., Pfister, G., Warner, J.X. (2013). Decadal record of satellite carbon monoxide observations. Atmos. Chem. Phys. 13(2), 837-850.

Xu, W.Y., Zhao, C.S., Ran, L., Deng, Z.Z., Liu, P.F., Ma, N., Lin, W.L., Xu, X.B., Yan, P., He, X., Yu, J., Liang, W.D., Chen, L.L. (2011). Characteristics of pollutants and their correlation to meteorological conditions at a suburban site in the North China Plain. Atmos. Chem. Phys., 11(9), 4353-4369.

Yurganov, L.N., Grechko, E.I., Dzhola, A.V. (1999). Zvenigorod carbon monoxide total column time series: 27-yr of measurements. Chemosphere Global Change Sci., 1(1-3), 127-136.

Yurganov, L., W. McMillan, E. Grechko, Dzhola, A. (2010). Analysis of global and regional CO burdens measured from space between 2000 and 2009 and validated by ground-based solar tracking spectrometers. Atmos. Chem. Phys. 10(8), 3479-3494.

Zander, R., Demoulin, P., Ehhalt, D.H., Schmidt, U., Rinsland, C.P. (1989). Secular increase of the total vertical column abundance of carbon monoxide above central Europe since 1950. J. Geophys. Res., 94(D8), 11,021-11,028.

Zellweger, C., Hüglin, C., Klausen, J., Steinbacher, M., Vollmer, M., Buchmann, B. (2009). Inter-comparison of four different carbon monoxide measurement techniques and evaluation of the long-term carbon monoxide time series of Jungfraujoch. Atmos. Chem. Phys., 9(11), 3491-3503.

Zhang, R., Wang, M., Ren, L. (2011). Long-term trends of carbon monoxide inferred using a two-dimensional model. Chemosphere Global Change Sci., 3(2), 123-132.

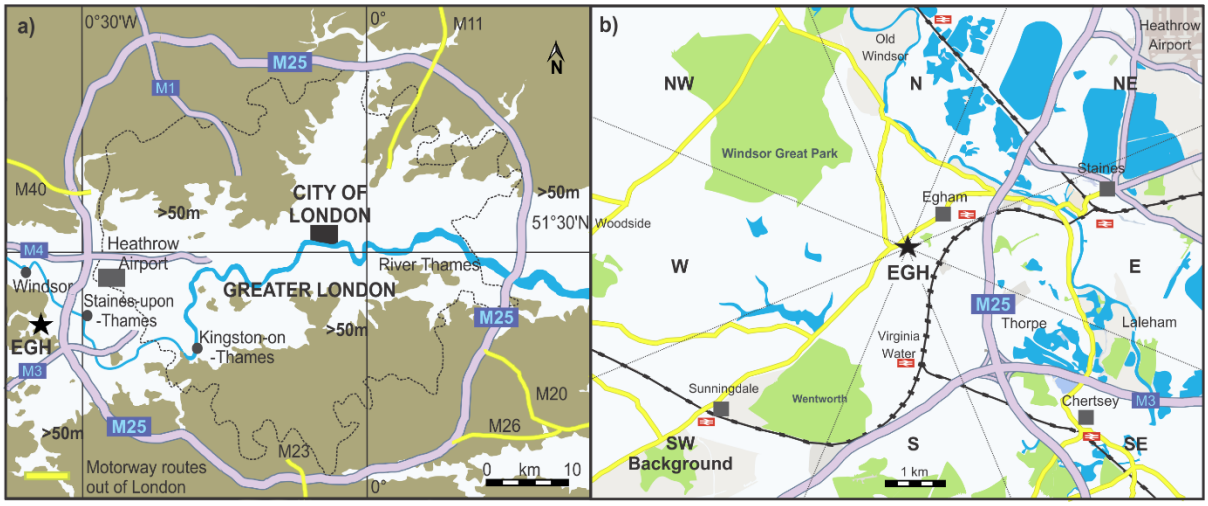

Fig. 1. a). Location of the EGH site and M25 motorway in relation to the Greater London area. b). EGH site and London motorway routes in the local context, and wind sectors definition. Adapted from: OpenStreetMap contributors (2015). Retrieved from https://planet.openstreetmap.org.

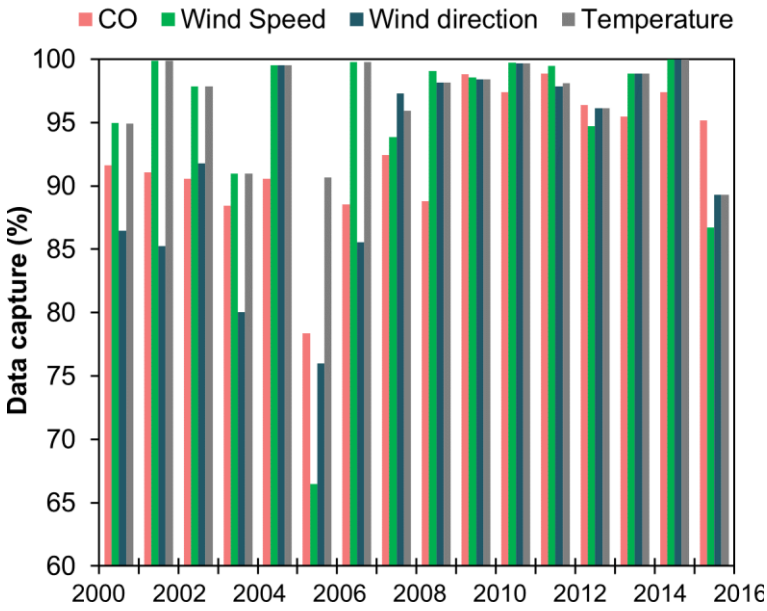

Fig. 2. Data capture of 30-min values for CO, wind speed, wind direction and temperature during 2000-2012 at EGH.

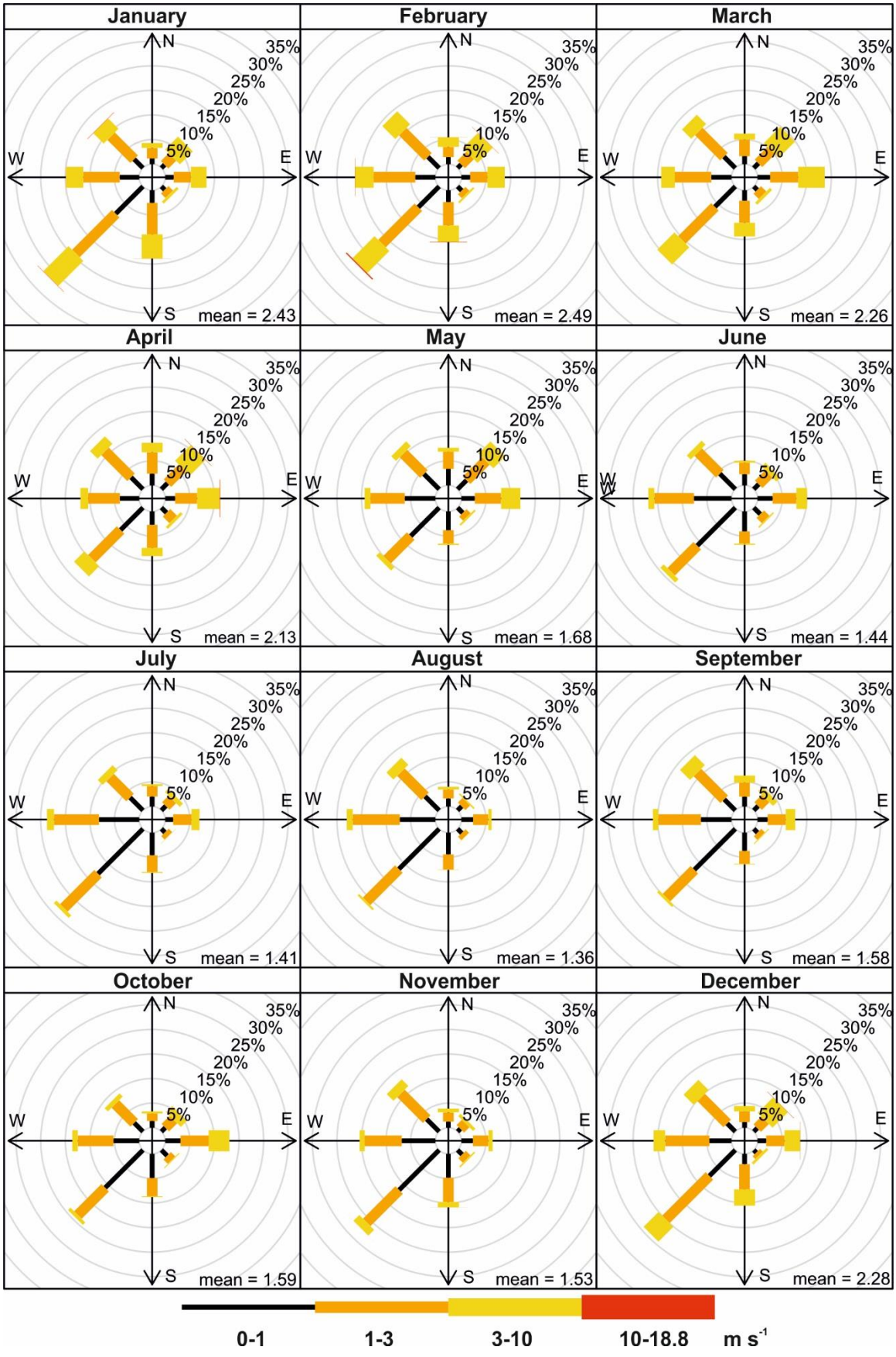

Fig. 3. Frequency of counts of measured wind direction occurrence by month at EGH during 2000-2015.

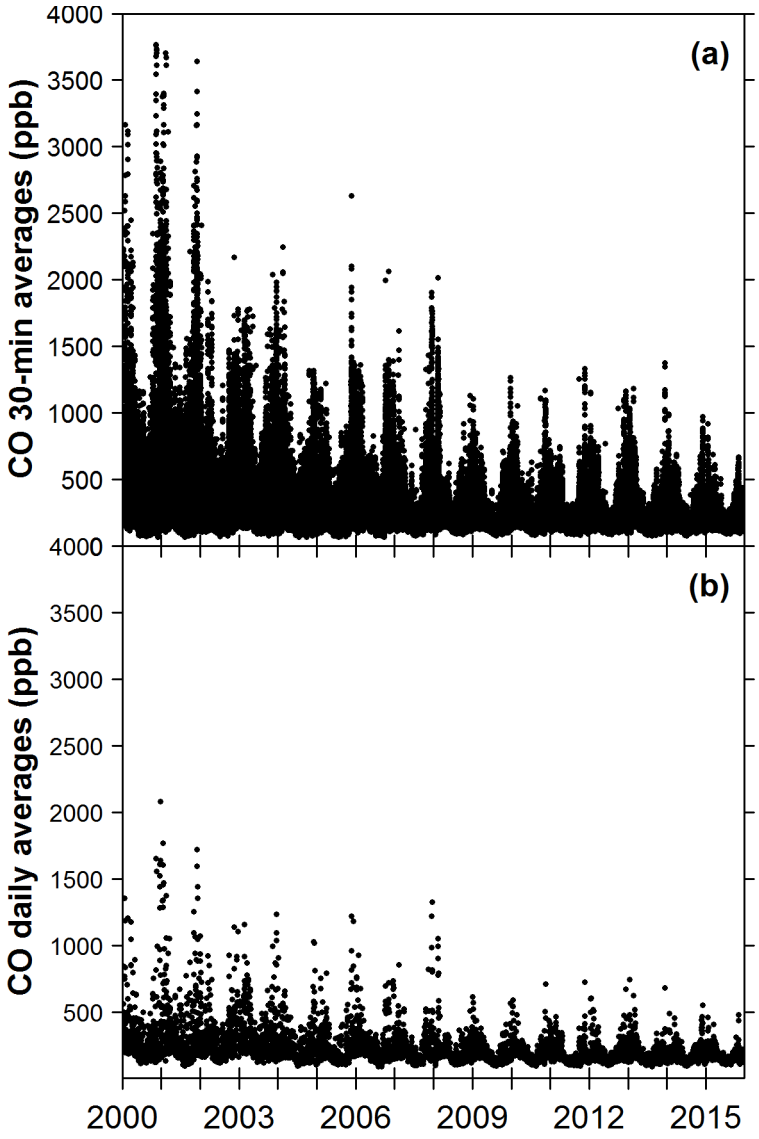

Fig. 4. a). 30-minute averages of CO during 2000-2012 at EGH. b). Daily averages during the same period.

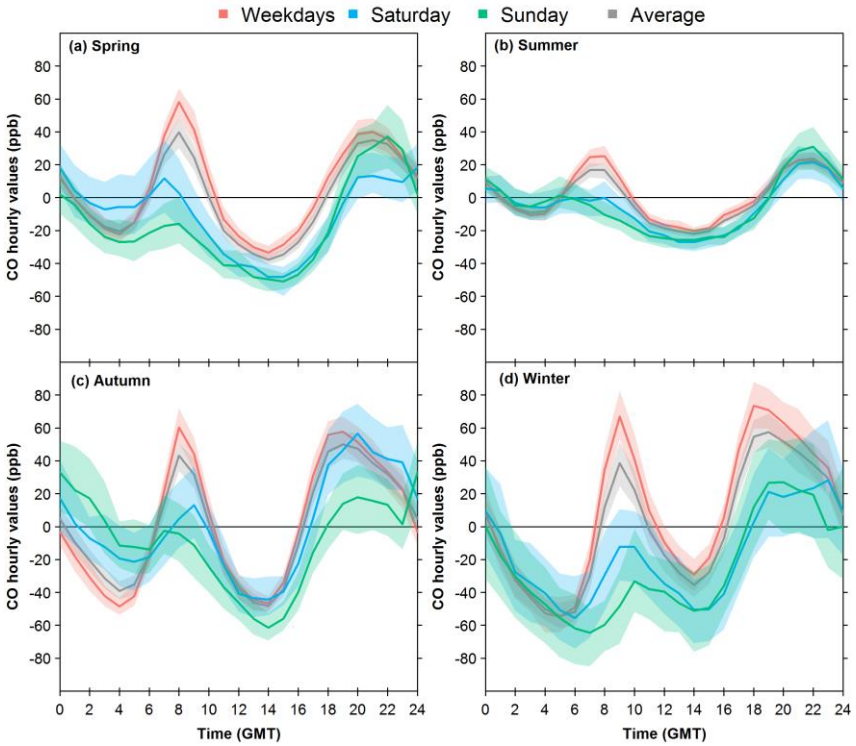

Fig. 5. CO normalised diurnal cycles by season at EGH during 2000-2015. The shadings show the 95 % confidence intervals of the averages calculated through bootstrap resampling (Carslaw, 2015).

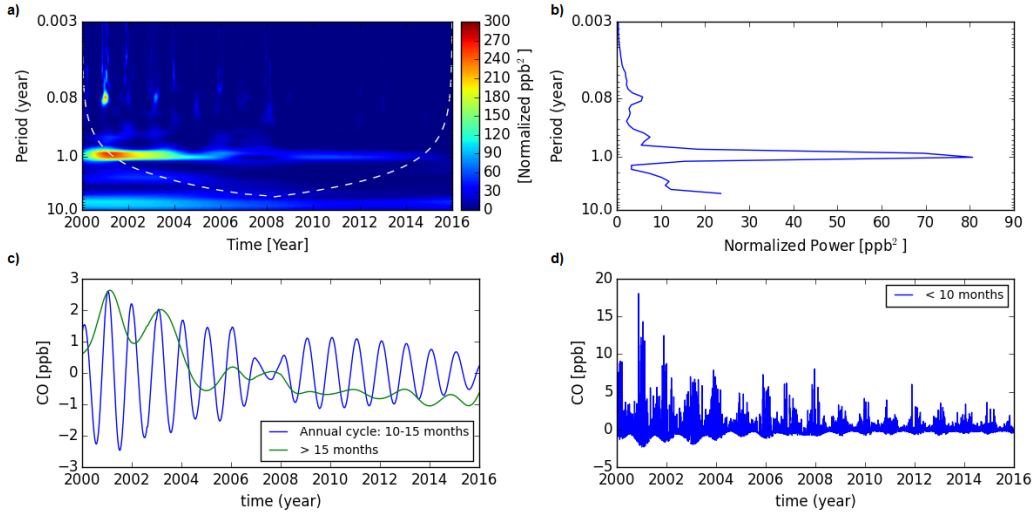

Fig. 6. Spectral de-composition of the CO data set recorded at EGH from 2000 to 2015. **a).** The wavelet power of the data, where warmer colours denote higher power. Values that sit below the cone of influence (white dashed line) are affected by edge effects and have a higher uncertainty and are not considered further, where 0.08 corresponds around to 1 month and 0.003 corresponds approximately to 1 day. **b).** The associated global wavelet spectrum, which represents a time integral of power. **c).** The seasonal (10-15 months), and low-variations (>15 months) and **d).** High-frequency variations (< 10 months) of CO as a function of time.

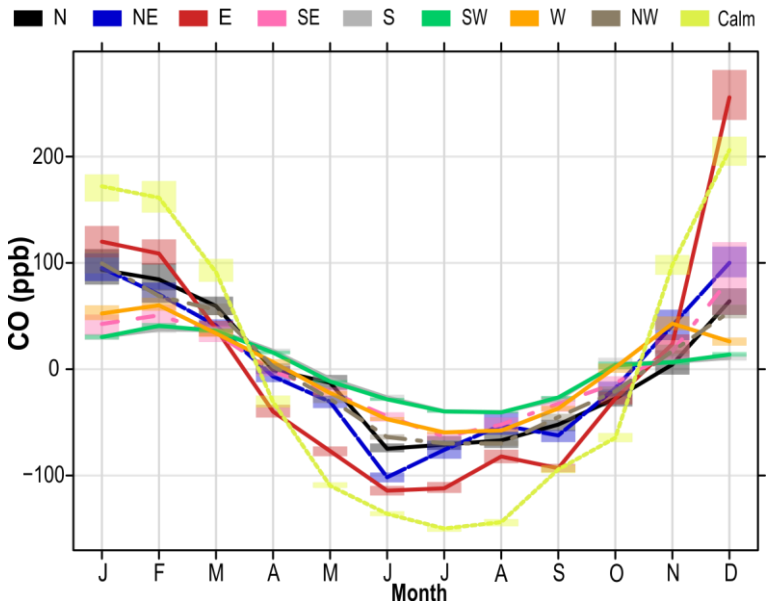

Fig. 7. De-trended average annual CO cycles by wind sector at EGH during 2000-2015. The shading shows the estimated 95 % confidence intervals estimated through bootstrap resampling (Carslaw, 2015).

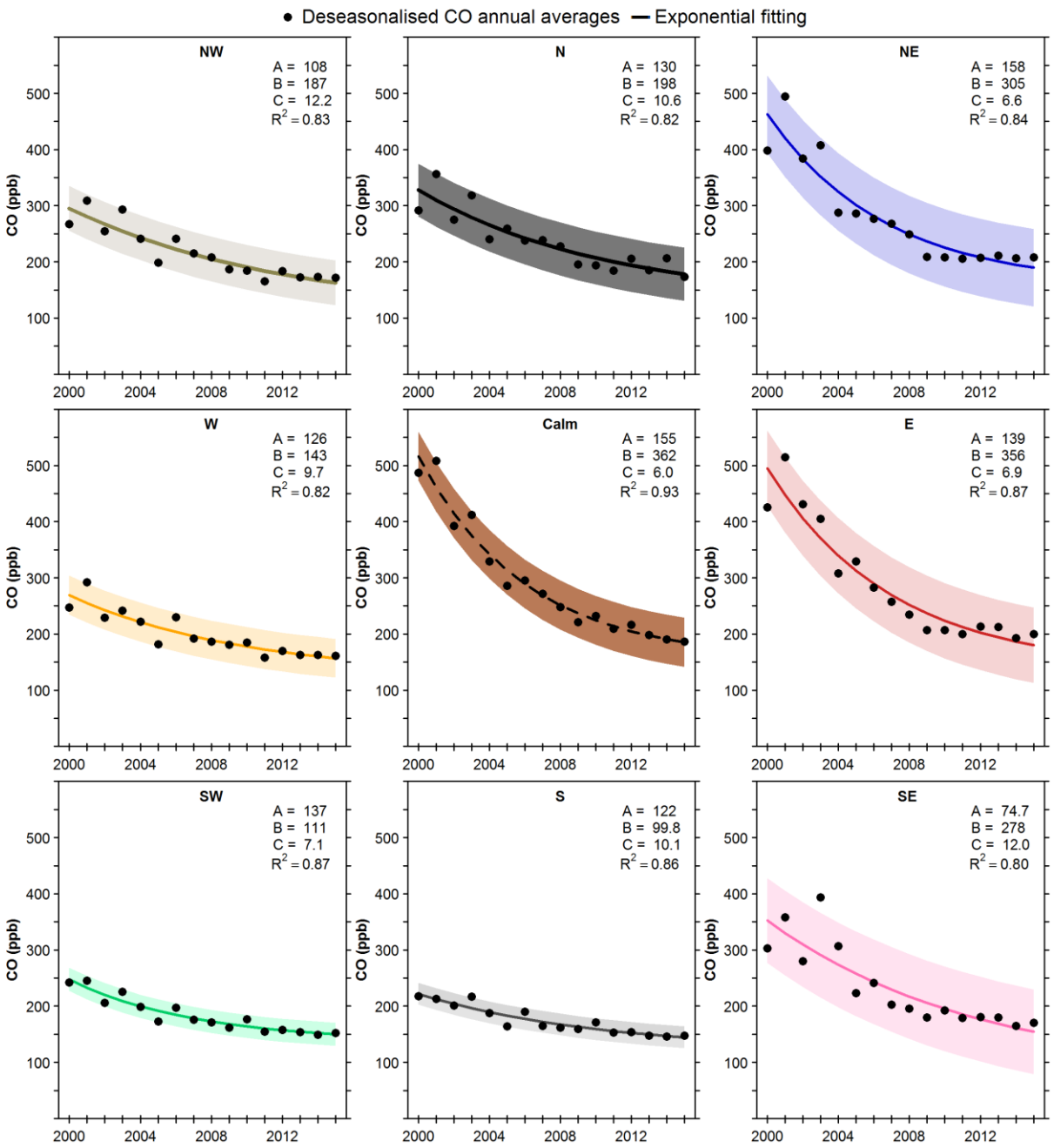

Fig. 8. Exponential decay in de-seasonalised annual averages of CO recorded at EGH by wind sector during 2000-2015. De-seasonalised annual averages were computed with the STL technique. The shading shows 95 % confidence intervals estimated through bootstrap resampling. As reported by Lowry et al. (2016), the best fit to the data are exponential curves to the de-seasonalised annual CO averages, with an offset exponential function of the form: $y = A + Be^{\frac{-(x-x_0)}{C}}$, where x_0 is the initial year of measurements, 2000. The parameters A, B and C, and the correlation coefficient for each wind sector are shown in their respective panels.

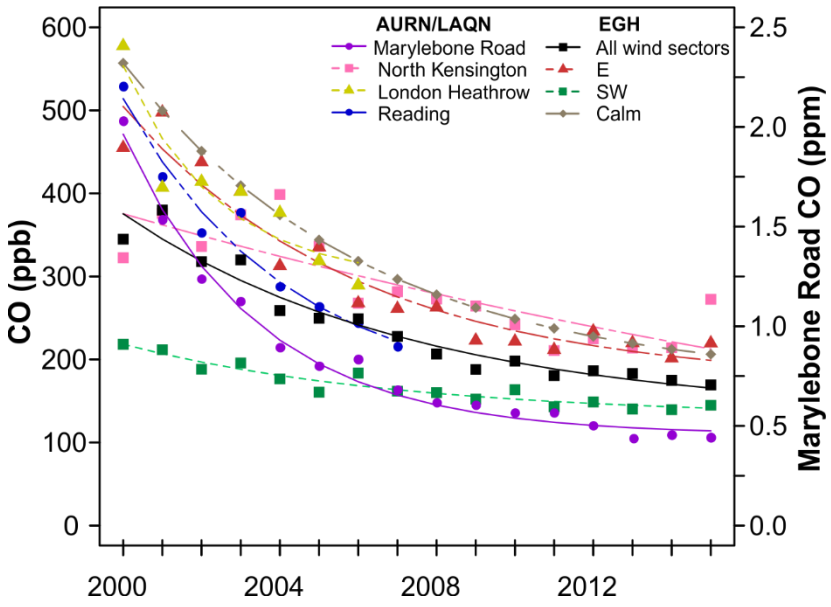

Fig. 9. Trends in CO ambient observed in SE England during 2000-2015 and comparison with changes in CO for the E, SW, calm and all wind sectors at EGH during the same period. LAQN site names LH2: Heathrow airport (closed 2011), MY1: Marylebone Road and REA: Reading (closed 2007). De-seasonalised annual averages were computed with the STL technique. The shading shows 95 % confidence intervals estimated through bootstrap resampling (Carslaw, 2015). As reported by Lowry et al. (2016), the best fit to the data are exponential curves to the de-seasonalised annual CO averages, with an offset exponential function of the form: $y = A + Be^{\frac{-(x-x_0)}{c}}$, where x_0 is the initial year of measurements, 2000.

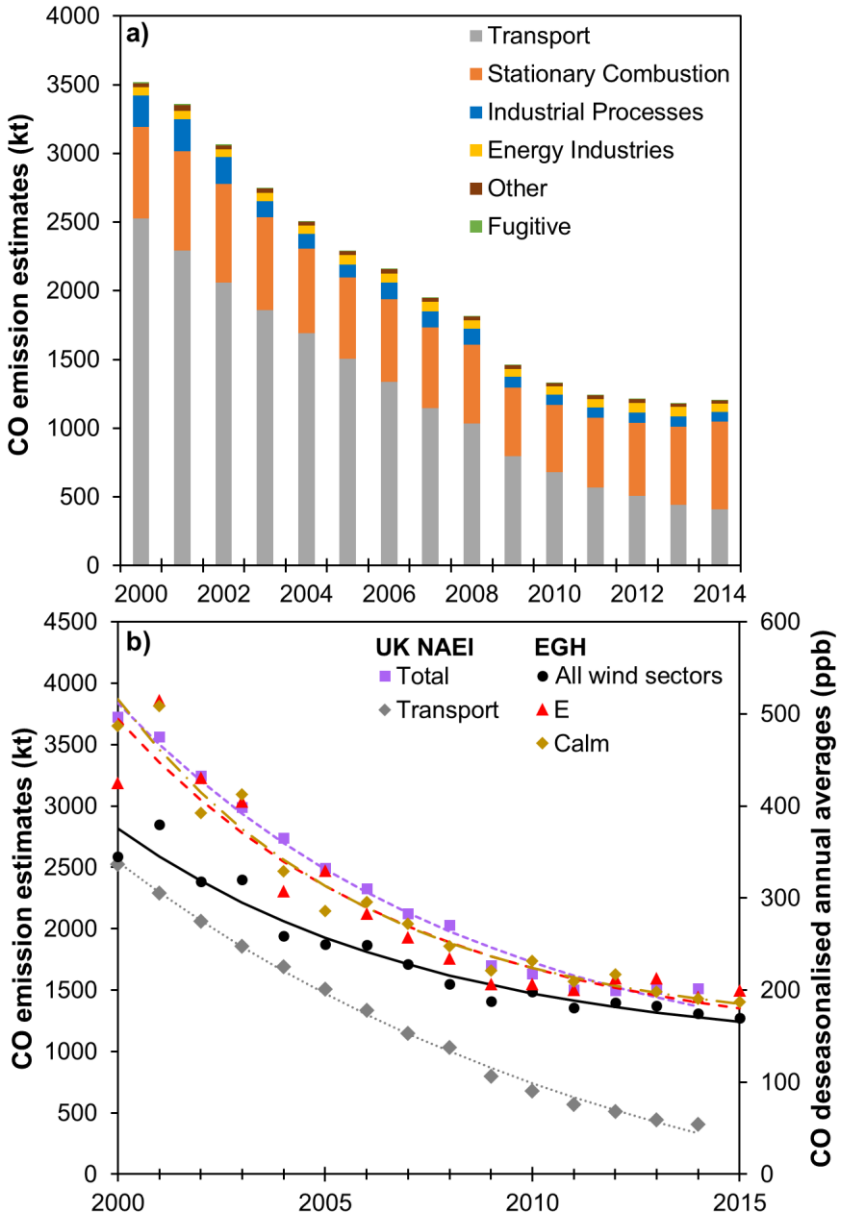

Fig. 10. (a) Trends in CO emissions during 2000-2014 in England by category as reported in the UK NAEI 2016. Stationary combustion is estimated as Industrial combustion + Residential combustion. (b) Comparison of the decay in CO estimated emissions as reported in the UK NAEI 2016 and CO measurements for all EGH wind sectors, E and calm during 2000-2015.

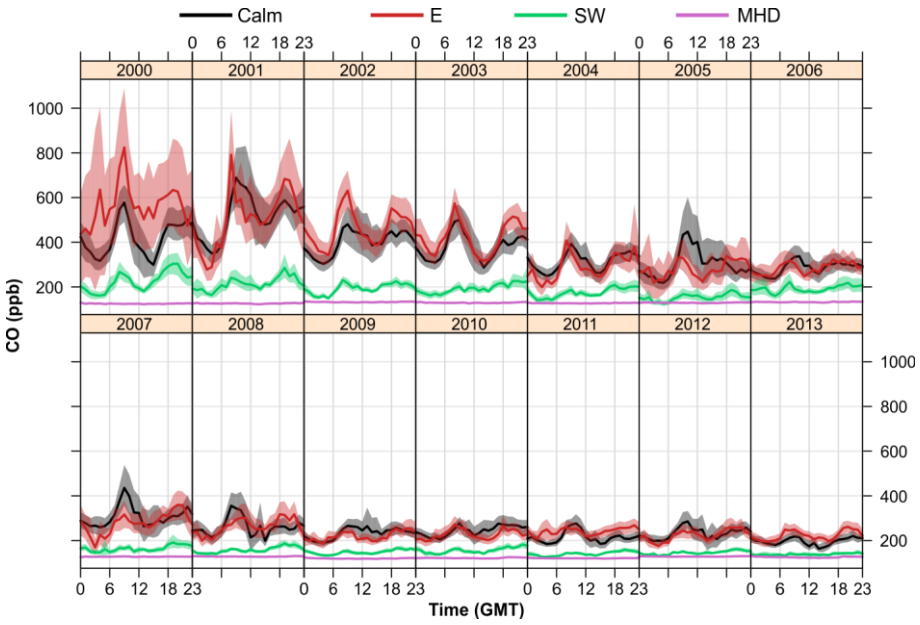

Fig. 11. CO diurnal cycles constructed from hourly averages at EGH and MHD during 2000-2013. The shading shows the estimated 95 % confidence intervals estimated through bootstrap resampling (Carslaw, 2015).

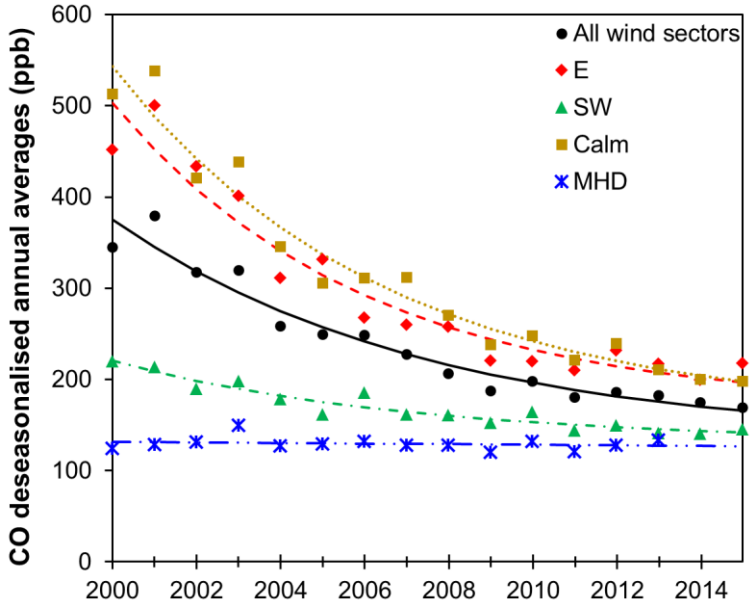

Fig. 12. Comparison between the exponential decay in CO for the E, SW, calm and all wind sectors at EGH during 2000-2015 with changes in CO at MHD during 2000-2013.

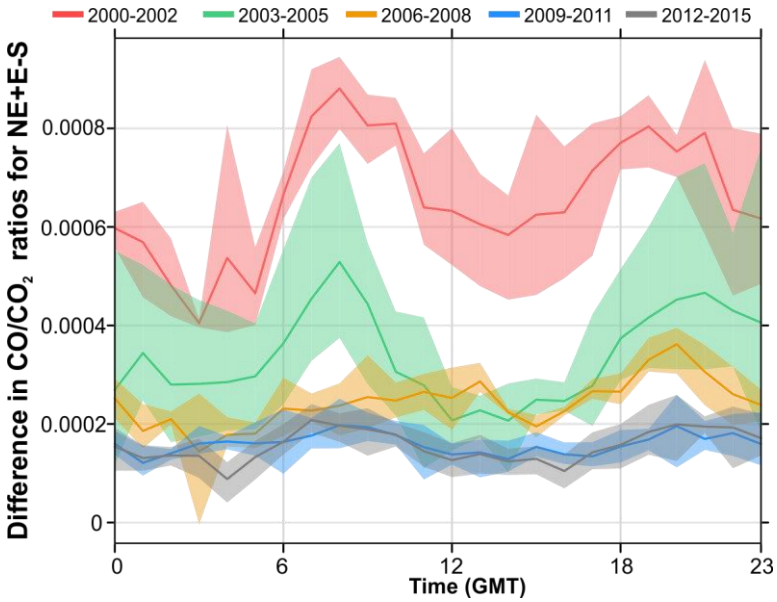

Fig. 13. Temporal analysis of the CO/CO_2 residual, i.e. the CO/CO_2 excess after subtracting S from NE-E wind sectors using a 1 h window data in the diurnal cycle. The shading shows the estimated 95 % confidence intervals estimated through bootstrap resampling (Carslaw, 2015).

Table 1. Monitoring sites description located in the Greater London Area and Reading used for CO long-term trends comparison with EGH data.

Monitoring site	QA/QC[a] standard	LAQN code	Classification	Operating period	Distance to road	Sampling height
Heathrow Airport	LAQN	LH2[b]	Industrial	1/1/1999 to 24/2/2011	N.A.	N.A.
Kensington and Chelsea – North Kensington	AURN/LAQN	KC1[c]	Urban Background	17/3/1995 to present	N.A.	3 m
Reading - New Town	AURN	RD0[c]	Urban Background	17/07/1997 to 30/09/2007	100 m	3 m
Westminster - Marylebone Road	AURN/ LAQN	MY1[c]	Kerbside	26/5/1997 to present	1.5 m	2.5 m

N.A.: Not applicable
[a]Quality Assurance and Quality Control standards
[b]Data not fully ratified for 2011
[c]Data ratified

Table 2. Statistics of CO 30-min data expressed in units of ppb recorded at EGH during 2000-2015.

Year	Average	SD	Median	Maximum
2000	343.3	109.5	238.5	3766.6
2001	386.1	141.4	265.6	3705.4
2002	318.3	99.4	236.3	2410.5
2003	324.9	92.5	243.7	2037.4
2004	255.0	79.2	199.7	2245.1
2005	254.3	97.4	183.4	2629.9
2006	239.6	59.3	199.0	2063.2
2007	228.6	82.8	180.8	1907.1
2008	208.9	64.2	171.6	1289.3
2009	185.7	48.7	161.0	1265.1
2010	197.8	55.9	173.9	1168.5
2011	178.7	52.1	151.5	1330.8
2012	186.7	42.2	159.3	1166.0
2013	183.1	51.0	153.3	1375.6
2014	175.1	45.2	150.7	988.9
2015	169.0	29.6	152.4	919.9

**Standard deviation of the annual averages calculated from monthly averages.*

Table 3. CO decline rates during 2000-2015 calculated by wind sector at EGH.

Wind sector*	N	NE	E	SE	S	SW	W	NW	Calm
ppb yr^{-1}	8.6	13.9	18.7	10.2	4.7	5.9	6.5	7.7	17.9
% yr^{-1}	2.9	3.8	4.8	3.7	2.4	2.7	2.8	3.0	4.6
Overall decline (%)	46.4	60.8	76.8	59.2	38.4	43.2	44.8	48.0	73.6

*All declines are significant at $p<0.001$.